AIP | Applied Physics Letters

Solution processable interface materials for nanoparticulate organic photovoltaic devices

Nicolas Nicolaidis, Ben Vaughan, Cara J. Mulligan, Glenn Bryant, Tino Zillger, Bystrik Trnovec, Arved C. Hübler, Natalie Holmes, Nathan A. Cooling, Matthew J. Griffith, Chhinder Bilen, Pankaj Kumar, Krishna Feron, Xiaojing Zhou, Daniel Elkington, Warwick J. Belcher, and Paul C. Dastoor

Citation: Applied Physics Letters **104**, 043902 (2014); doi: 10.1063/1.4863216
View online: http://dx.doi.org/10.1063/1.4863216
View Table of Contents: http://scitation.aip.org/content/aip/journal/apl/104/4?ver=pdfcov
Published by the AIP Publishing

Solution processable interface materials for nanoparticulate organic photovoltaic devices

Nicolas Nicolaidis,[1,2] Ben Vaughan,[1,2] Cara J. Mulligan,[1] Glenn Bryant,[1] Tino Zillger,[3] Bystrik Trnovec,[3] Arved C. Hübler,[3] Natalie Holmes,[1] Nathan A. Cooling,[1] Matthew J. Griffith,[1] Chhinder Bilen,[1] Pankaj Kumar,[1,4] Krishna Feron,[1] Xiaojing Zhou,[1] Daniel Elkington,[1] Warwick J. Belcher,[1] and Paul C. Dastoor[1,a)]
[1]*Centre for Organic Electronics, University of Newcastle, Callaghan, NSW 2308, Australia*
[2]*CSIRO Energy Technology, P. O. Box 330, Newcastle, NSW 2300, Australia*
[3]*Institute for Print and Media Technology, Chemnitz University of Technology, Chemnitz D-09126, Germany*
[4]*CSIR-National Physical Laboratory, Dr. K. S. Krishnan Marg, New Delhi 110012, India*

(Received 16 December 2013; accepted 10 January 2014; published online 28 January 2014)

Nanoparticulate zinc oxide can be prepared at low temperatures from solution processable zinc acetylacetonate. The use of this material as a cathode interfacial layer in nanoparticulate organic photovoltaic devices results in comparable performances to those based on reactive calcium layers. Importantly, the enhanced degradation stability and full solution processability make zinc oxide a more desirable material for the fabrication of large area printed devices. © *2014 AIP Publishing LLC*. [http://dx.doi.org/10.1063/1.4863216]

The morphology of the blended components plays a key role in determining the device performance in organic solar cells.[1–3] Moreover, the use of non-toxic solvents is essential for commercial production to ensure environmental and occupational health and safety compliance.[4,5] Aqueous nanoparticulate (NP) dispersions of polymer and fullerene materials fulfil both of these requirements.[6,7] However, if nanoparticulate dispersions are to become more readily adopted for active layer production, they will need to preserve device performance stability whilst maintaining suitability for large area coating techniques such as reel-to-reel printing. Nanoparticulate device performance is improved by the addition of a thin calcium layer between the active layer and aluminium cathode,[8,9] consistent with the improvement that occurs in standard bulk heterojunction (BHJ) devices.[10,11] However, the use of Ca layers with water-dispersed NPs in printed devices is problematic, since the instability of Ca to retained water is likely to limit its applicability in commercial scale organic solar cell production.[12] As such, an alternative interface layer (IL) that is better suited to solution based processing with improved resistance to oxidative degradation and/or hydrolysis is urgently required. In this Letter, we present zinc acetylacetonate ($Zn(acac)_2$) as an interfacial layer in NP organic photovoltaic (NPOPV) devices. $Zn(acac)_2$ shows great promise as a cathode interface precursor, since it is solution processable and is readily converted at low temperatures (~120 °C) to more stable zinc oxide (ZnO) nanoparticles. However, this approach has yet to be implemented in NPOPV devices. We show that a ZnO cathode interface layer produced via a $Zn(acac)_2$ precursor provides a similar improvement in device performance to that provided by a calcium layer, whilst retaining the twin benefits of increased stability and compatibility with reel-to-reel coating techniques.

In order to determine whether the low temperature solution processed ZnO layer is a suitable replacement for Ca as a device interfacial layer in NPOPVs, a series of devices were fabricated and characterised.[13] Figure 1(a) shows the schematic architecture of these devices, which comprise a P3HT:PCBM NP active layer, incorporating a thin IL of ZnO or Ca underneath an Al cathode layer. Devices were also studied with a bare Al cathode without any interface layer.

A key difference between the cathode structures lies in their electronic properties, which are illustrated in Figure 1(b). The work function for aluminium is commonly reported to be 4.3 eV,[14] but for NPOPV devices, residual water in the active layer (which can be observed in the differential scanning calorimetry of the NPs[15]) is likely to result in oxidation of the aluminium cathode and the formation of an interfacial oxide layer. The work function of a native layer of aluminium oxide on aluminium has been reported to be 3.8 eV;[16] however, for hydroxylated alumina interfaces, the work function rises to 4.3 eV.[17,18] Consequently, in a NPOPV device, both pristine and oxidised aluminium electrodes will have similar work functions (4.2–4.3 eV), although the series resistance (R_s) of the degraded cathode will be higher.[19]

The work function for pristine calcium is 2.89 eV,[20] whereas the work function of calcium oxide has been reported as 1.69 eV.[21] Thus, the driving force for electron transport across a standard Ca/Al electrode in OPVs is not dictated by the work function of the thin (~20 nm) Ca layer. Indeed, devices fabricated with a thick (>30 nm) Ca layer protected by a thin Al coating show a considerable reduction in performance due to the lower Ca work function dominating the interfacial energetics.[20] Hence, calcium interfacial layers are necessarily thin, since an incomplete layer is required for optimal device performance (and thus the electrode work function is not pinned to Ca/CaO). Furthermore, although the CaO will have a higher resistivity than pristine Ca,[22,23] the incomplete/porous nature of the degraded Ca

a)Tel.:+61-2-4921 5426. Fax: +61-2-4921 6907. Email: Paul.Dastoor@newcastle.edu.au

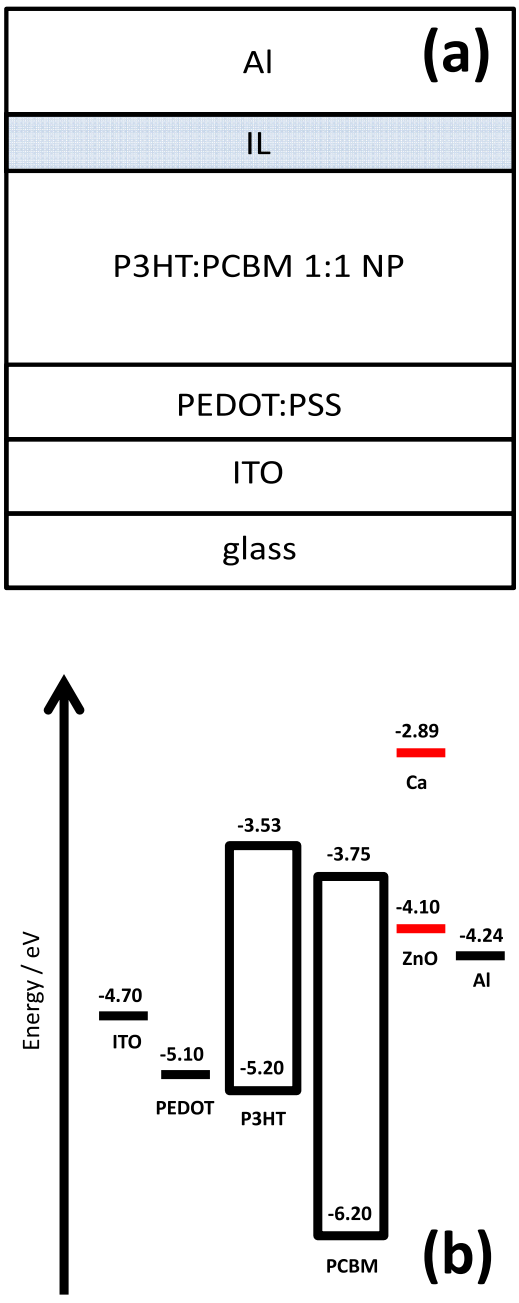

FIG. 1. (a) Device architecture of NPOPV devices, with a thin IL of ZnO or Ca underneath an Al cathode. (b) Energy level diagram for the different NPOPV device architectures.

layer means that this will not dominate the overall R_s of the device.[24]

By comparison, the work function of ZnO is 4.1 eV and thus well suited for charge injection from PCBM and into the Al cathode. Whilst UV treatment of such ZnO layers is typically used to increase the conductivity of the layer (via loss of O_2^- radicals) and results in a decrease in work function of the ZnO layer from 4.2 eV to 3.7 eV, this decrease is only temporary and does not determine the work function of the interface.[25] Therefore, the application of solution processed ZnO appears to be an attractive route for the replacement of reactive Ca interfacial layers in NPOPV devices.

The use of a $Zn(acac)_2$ precursor solution provides a versatile method for producing ZnO NP layers *in-situ* via a low temperature ligand exchange process and subsequent heat treatment[26] and thus is well-suited to printing-based fabrication. Figures 2(a) and 2(b) show the atomic force microscopy (AFM) images of spin coated $Zn(acac)_2$ precursor and thermally converted ZnO NP films, respectively. From a particle size analysis of the images (Figure 2(c)), we see that the mean particle size in the precursor and ZnO films is 80–100 nm, consistent with the previous reports.[26] Furthermore, from

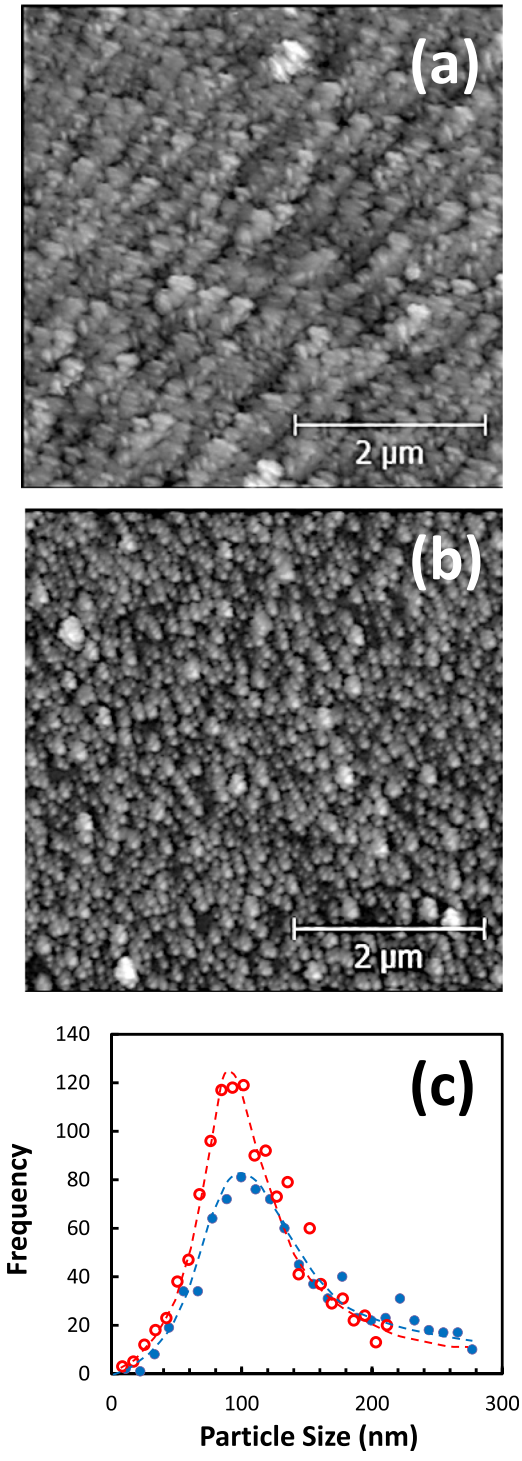

FIG. 2. Atomic force microscope images of the $Zn(acac)_2$ precursor film (a) and thermally converted ZnO film (b). The contrast greyscale corresponds to a maximum height difference of 200 nm in both cases. Panel (c) shows the particle size distribution obtained from the AFM images of precursor (solid blue circles) and the thermally converted ZnO (open red circles) films. A dashed line has been added to guide the eye in both cases.

TABLE I. Photovoltaic performance parameters measured for best annealed P3HT:PCBM nanoparticulate devices with different cathode structures.

Cathode structure	V_{oc} (mV)	J_{sc} (mA cm^{-2})	FF	η (%)
Al	336	1.52	0.369	0.188
ZnO/Al	434	2.25	0.359	0.351
Ca/Al	457	3.23	0.398	0.587

Figure 2(b), it is clear that the ZnO films form a well packed layer with a particle size that is about twice that of the P3HT:PCBM NPs (30–40 nm).[7]

Table I shows the device parameters for the best devices fabricated for the three cathode architectures.[13] It is clear from this data that the device with a Ca interfacial layer performs better than that with a ZnO interfacial layer, with the Al-only cathode performing worst. Furthermore, the differences in performance arise primarily from systematic changes in J_{sc} and V_{oc}.

Figure 3(a) shows the corresponding J-V curves for the NPOPV devices with the three different cathode structures and highlights that the major difference between the Ca/Al and ZnO/Al devices lies in the J_{sc} value, which is higher for the Ca/Al device. Figure 3(b) shows the external quantum efficiency (EQE) characteristics of the devices and reveals that, while the Ca/Al and ZnO/Al devices exhibit near identical profiles, the Al device displays an EQE spectrum that is significantly different. Recent work by Gevaerts *et al*. has shown that the shape of the EQE plot reflects the degree of vertical phase segregation present in P3HT:PCBM devices.[27] In particular, as the P3HT component becomes more segregated so the EQE in the region of maximum P3HT absorption is depressed (via a "filter effect"[28]). As shown in Figure 3(c), the region of reduced EQE in the Al cathode device corresponds to the absorption profile of the P3HT in the NP active layer. Nicolaidis *et al*. have shown that the proportion of photocurrent generated by each component is directly reflected in the EQE spectrum.[29] Thermal annealing of P3HT:PCBM bulk heterojunction devices is known to result in significant changes to device morphology and, in particular, vertical phase segregation of the components.[30] As such, we speculate that annealing of the Al cathode device results in some phase segregation of the components in the P3HT:PCBM NP layer producing regions of high purity P3HT in which photocurrent generation is reduced. Furthermore, consistent with this hypothesis, unannealed Al cathode devices measured for this study exhibit higher J_{sc} values.[13] Interestingly, this phase segregation does not appear to occur in the Ca/Al or the ZnO/Al devices, suggesting that the free energies of interface formation driving diffusion of the components are significantly different to that of the Al cathode. Figure 3(d) shows the variation in J_{sc} as a function of incident light intensity and by fitting a power law relationship to the data, information relating to the space charge characteristics in the device can be inferred.[31] The exponent of the power law fits ranges from 0.77 to 0.80, close to the ideal value of 0.75 for a space charge limited device.[32] Thus, it would appear that regardless of cathode structure, all of the NPOPV devices are space-charge limited.

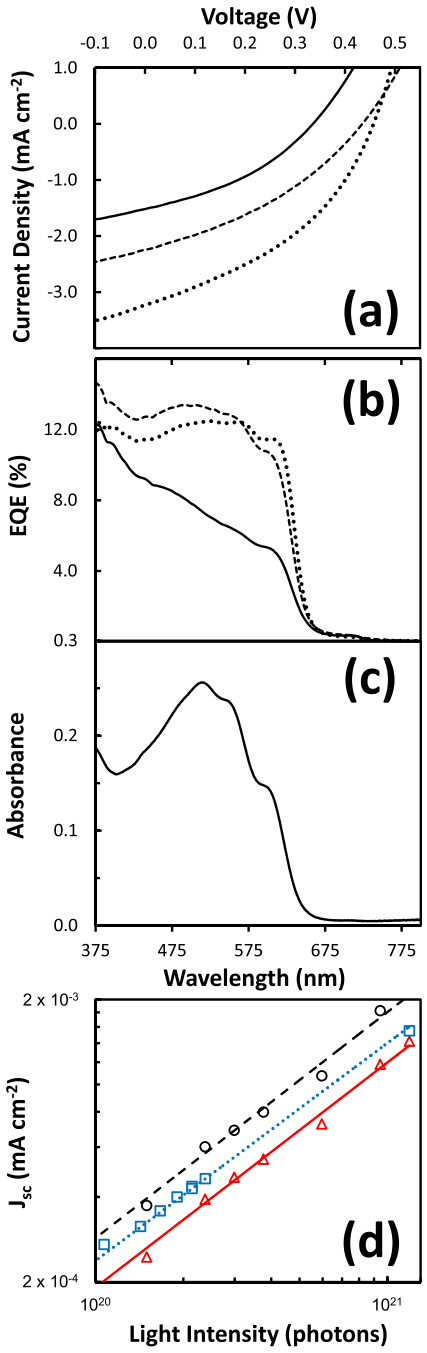

FIG. 3. (a) Current density versus voltage characteristics for devices with Al (solid line), ZnO/Al (dashed line), and Ca/Al (dotted line) cathode structures. (b) External quantum efficiency versus wavelength for devices with Al (solid line), ZnO/Al (dashed line), and Ca/Al (dotted line) cathode structures. (c) UV-vis absorbance spectrum for P3HT:PCBM NP film. (d) Short circuit current density versus light intensity for devices with Al (solid line and red triangles), ZnO/Al (dashed line and black circles), and Ca/Al (dotted line and blue squares) cathode structures. The linear fits are $2.23 \times 10^{-20}x^{0.797}$, $2.82 \times 10^{-20}x^{0.800}$, and $9.20 \times 10^{-20}x^{0.771}$ for the Al, ZnO/Al, and Ca/Al cathode, respectively.

In summary, we have shown that using the low temperature $Zn(acac)_2$ pathway results in a ZnO cathode interfacial layer, which can replace conventional Ca layers with little or no loss of NPOPV device performance. Indeed, these results suggest that preformed and stable ZnO nanoparticle inks that are used for reel-to-reel manufacture today[33] are also likely to function as buffer layers in NPOPV devices. Moreover,

given that the devices presented in this work have been fabricated and treated post-fabrication, using conditions which are optimal for the Ca/Al cathode, means that considerable improvement of the ZnO/Al cathode devices may be expected through optimisation of this new architecture. This observation, coupled with the advantageous low temperature solution processability of the ZnO and the improved stability of this layer to oxidative degradation, makes further investigation of NPOPVs with ZnO/Al cathodes warranted.

Special thanks to the University of Newcastle Electron Microscopy and X-ray Unit. The University of Newcastle and the Australian Renewable Energy Agency (ARENA) are gratefully acknowledged for Ph.D. scholarships (N.H., N.N., C.M.). This project was supported by the Australian Government, through the Australian Renewable Energy Agency (K.F.). The Australia-Germany Solar Photovoltaics Research Program (part of the International Science Linkages (ISL) program) is gratefully acknowledged for travel funding (N.N., C.M., G.B., and P.D.). One of the authors (P.K.) is grateful to Indian National Science Academy (INSA), New Delhi, for the award of an Early Career Indo-Australia research fellowship to pursue this work in Australia. This work was performed in part at the Materials node of the Australian National Fabrication Facility, a company established under the National Collaborative Research Infrastructure Strategy to provide nano and microfabrication facilities for Australia's researchers.

[1]L. M. Chen, Z. Hong, G. Li, and Y. Yang, Adv. Mater. **21**, 1434 (2009).
[2]T. Wang, A. D. F. Dunbar, P. A. Staniec, A. J. Pearson, P. E. Hopkinson, J. E. MacDonald, S. Lilliu, C. Pizzey, N. J. Terrill, A. M. Donald, A. J. Ryan, R. A. L. Jones, and D. G. Lidzey, Soft Matter **6**, 4128 (2010).
[3]X. Yang and J. Loos, Macromolecules **40**, 1353 (2007).
[4]A. M. Ruder, Ann. NY Acad. Sci. **1076**, 207 (2006).
[5]E. M. Ward, P. A. Schulte, K. Straif, N. B. Hopf, J. C. Caldwell, T. Carreón, D. M. DeMarini, B. A. Fowler, B. D. Goldstein, K. Hemminki, C. J. Hines, K. H. Pursiainen, E. Kuempel, J. Lewtas, R. M. Lunn, E. Lynge, D. M. McElvenny, H. Muhle, T. Nakajima, L. W. Robertson, N. Rothman, A. M. Ruder, M. K. Schubauer-Berigan, J. Siemiatycki, D. Silverman, M. T. Smith, T. Sorahan, K. Steenland, R. G. Stevens, P. Vineis, S. H. Zahm, L. Zeise, and V. J. Cogliano, Environ. Health Perspect. **118**, 1355 (2010).
[6]T. R. Andersen, T. T. Larsen-Olsen, B. Andreasen, A. P. L. Böttiger, J. E. Carlé, M. Helgesen, E. Bundgaard, K. Norrman, J. W. Andreasen, M. Jørgensen, and F. C. Krebs, ACS Nano **5**, 4188 (2011).
[7]N. P. Holmes, K. B. Burke, P. Sista, M. Barr, M. C. Stefan, A. L. D. Kilcoyne, X. Zhou, P. C. Dastoor, and W. J. Belcher, Sol. Energy Mater. Sol. Cell **117**, 437 (2013).
[8]B. Vaughan, A. Stapleton, B. Xue, E. Sesa, X. Zhou, G. Bryant, W. Belcher, and P. Dastoor, Appl. Phys. Lett. **101**, 053901 (2012).
[9]S. Ulum, N. Holmes, D. Darwis, K. Burke, A. L. D. Kilcoyne, X. Zhou, W. Belcher, and P. Dastoor, Sol. Energy Mater. Sol. Cell **110**, 43 (2013).
[10]C. M. Ramsdale, J. A. Barker, A. C. Arias, J. D. MacKenzie, R. H. Friend, and N. C. Greenham, J. Appl. Phys. **92**, 4266 (2002).
[11]C. J. Brabec, A. Cravino, D. Meissner, N. S. Sariciftci, T. Fromherz, M. T. Rispens, L. Sanchez, and J. C. Hummelen, Adv. Funct. Mater. **11**, 374 (2001).
[12]S. Cros, M. Firon, S. Lenfant, P. Trouslard, and L. Beck, Nucl. Instrum. Methods Phys. Res. B **251**, 257 (2006).
[13]See supplementary material at http://dx.doi.org/10.1063/1.4863216 for experimental details; corresponding data for the average device parameters for a minimum of twelve devices, as well as associated errors estimated by standard deviation; and unannealed device characteristics.
[14]M. Girtan and M. Rutu, Sol. Energy Mater. Sol. Cell **94**, 446 (2010).
[15]A. Stapleton, B. Vaughan, B. Xue, E. Sesa, K. Burke, X. Zhou, G. Bryant, O. Werzer, A. Nelson, A. L. D. Kilcoyne, L. Thomsen, E. Wanless, W. Belcher, and P. Dastoor, Sol. Energy Mater. Sol. Cell **102**, 114 (2012).
[16]Y. Vaynzof, T. J. Dennes, J. Schwartz, and A. Khan, Appl. Phys. Lett. **93**, 103305 (2008).
[17]R. A. Chapman, J. Appl. Phys. **35**, 2832 (1964).
[18]E.-G. Kim and J.-L. Brédas, Org. Electron. **14**, 569 (2013).
[19]E. Voroshazi, B. Verreet, T. Aernouts, and P. Heremans, Sol. Energy Mater. Sol. Cell **95**, 1303 (2011).
[20]Y. S. Eo, H. W. Rhee, B. D. Chin, and J.-W. Yu, Synth. Met. **159**, 1910 (2009).
[21]B. J. Hopkins and F. A. Vick, Br. J. Appl. Phys. **9**, 257 (1958).
[22]G. W. C. Kaye and T. H. Laby, *Tables of Physical and Chemical Constants*, 15th ed. (Longman, Essex, UK, 1986).
[23]N. A. Surplice, Br. J. Appl. Phys. **17**, 175 (1966).
[24]M. T. Lloyd, D. C. Olson, P. Lu, E. Fang, D. L. Moore, M. S. White, M. O. Reese, D. S. Ginley, and J. W. P. Hsu, J. Mater. Chem **19**, 7638 (2009).
[25]P. de Bruyn, D. J. D. Moet, and P. W. M. Blom, Org. Electron. **11**, 1419 (2010).
[26]G. Ambrožič, S. D. Škapin, M. Žigon, and Z. C. Orel, Mater. Res. Bull. **46**, 2497 (2011).
[27]V. S. Gevaerts, L. J. A. Koster, M. M. Wienk, and R. A. J. Janssen, ACS Appl. Mater. Interfaces **3**, 3252 (2011).
[28]M. G. Harrison, J. Grüner, and G. C. W. Spencer, Phys. Rev. B **55**, 7831 (1997).
[29]N. Nicolaidis, B. Routley, J. Holdsworth, W. Belcher, X. Zhou, and P. Dastoor, J. Phys. Chem. C **115**, 7801 (2011).
[30]B. Xue, B. Vaughan, C.-H. Poh, K. B. Burke, L. Thomsen, A. Stapleton, X. Zhou, G. W. Bryant, W. Belcher, and P. C. Dastoor, J. Phys. Chem. C **114**, 15797 (2010).
[31]V. Mihailetchi, J. Wildeman, and P. Blom, Phys. Rev. Lett. **94**, 126602 (2005).
[32]P. W. M. Blom, V. D. Mihailetchi, L. J. A. Koster, and D. E. Markov, Adv. Mater. **19**, 1551 (2007).
[33]M. Hösel, R. R. Søndergaard, M. Jørgensen, and F. C. Krebs, Energy Technol. **1**, 102 (2013).